Influence of Monomer Structure and Dose Rate on Kinetic Elements in Electron-beam Polymerizations

Nicole L. K. Thiher
Department of Chemical & Biochemical Engineering, University of Iowa, Iowa City, IA 52242 USA
nicole-kloepfer@uiowa.edu

Sage M. Schissel
PCT Ebeam and Integration, LLC, Davenport, IA 52806
sage.schissel@pctebi.com

Julie L. P. Jessop
School of Chemical Engineering, Mississippi State University, Mississippi State, MS 39762 USA
jessop@che.msstate.edu

Abbreviations:

α – fractional conversion
αDRE – dose rate effect in conversion
ΔE – energy required to abstract each hydrogen on a monomer
ρ – density
BA – benzyl acrylate
CHA – cyclohexyl acrylate
D – dose
DDA – dodecyl acrylate
DMA – dynamic mechanical analysis
DPPH – 2,2,1-diphenyl-1-picrylhydrazyl
DRE – dose rate effect
EB – electron beam
EEEA – 2-(2-ethoxyethoxy)ethyl acrylate
$G(M^{\bullet})$ – initiating radical radiation chemical yield
$G(R^{\bullet})$ – primary radical radiation chemical yield
G-value – radiation chemical yield
HPOPA – 2-hydroxy-3-phenoxypropyl acrylate
$I_{ref}(M)$ – peak intensity of the reference peak of the monomer
$I_{rxn}(M)$ – peak intensity of the reaction peak of the monomer
$I_{ref}(P)$ – peak intensity of the reference peak of the polymer
$I_{rxn}(P)$ – peak intensity of the reaction peak of the polymer
k_i – initiation rate constant
k_p – propagation rate constant
k_{tp} – primary termination rate constant
M – monomer
$M^{\bullet}$ – initiating radical
MW – molecular weight
PA – phenyl acrylate
PEA – 2-phenylethyl acrylate
PET – polyethylene terephthalate
POEA – 2-phenoxyethyl acrylate
$R^{\bullet}$ – primary radical
R_p – rate of polymerization
R_R – rate of radical formation
t – time
T_g – glass transition temperature
T_gDRE – dose rate effect in glass transition temperature

Influence of Monomer Structure and Dose Rate on Kinetic Elements in Electron-beam Polymerizations

Nicole L. K. Thiher,[1] Sage M. Schissel,[2] Julie L. P. Jessop[3]

[1]University of Iowa, Chemical and Biochemical Engineering Department, Iowa City, IA

[2]PCT Ebeam and Integration, LLC, Davenport, IA

[3]Mississippi State University, School of Chemical Engineering, Mississippi State, MS

Abstract

In electron-beam (EB) polymerizations, altering the dose rate can cause property changes in the cured polymer, such as conversion, glass transition temperature (T_g), and physical or mechanical properties. These dose rate effects (DREs) complicate scale-up of EB polymerizations in industrial processes. A predictive relationship between DRE and changes in T_g was used to determine that DREs correlate to the number and lability of available bonds, not monomer size. Furthermore, the relationship between the primary radicals produced during EB irradiation and dose rate was explored via measurement of primary radical radiation chemical yield, $G(R^{\bullet})$. Namely, $G(R^{\bullet})$ is independent of dose rate, and instantaneous primary radical concentration is directly proportional to dose rate. Moreover, it was shown that non-reciprocity between dose rate and the rate of polymerization results in DREs. Future developments in radiation chemical yield measurements will aid in determining whether this disproportionality is due to the impact of dose rate on the concentration of propagating radicals or on the kinetic mechanism itself.

Keywords: dose rate effect, acrylate, radical concentration, rate of polymerization, radiation chemical yield, hydrogen abstraction

1. Introduction

Electron-beam (EB) polymerization is used to produce millions of tons of film, ink, coating, and adhesive products each year (Cohen, 2012). EB polymerization requires less energy and no solvents, making it more environmentally friendly compared to traditional thermal

polymerization processes (Kinstle, 1990). Furthermore, EB requires no initiator molecule and is not hindered by pigments and fillers, which can be problematic during photopolymerization (Wilson, 1974).

Despite these advantages, there are challenges that have limited the growth of EB technology. One such challenge arises during scale-up from a lab-scale EB unit or pilot line to an industrially sized EB. The dose (*i.e.*, the energy absorbed by the sample) of small and large scale EB units are often comparable, but the speed at which the dose is delivered – dose rate – changes. Altering the dose rate can cause property changes in the cured polymer, known as dose rate effects (DREs). Changes in conversion, glass transition temperature (T_g), and physical or mechanical properties have been observed during EB polymerization as the result of altering the dose rate used to create polymer films (Rangwalla and Nablo, 1990; Xiancong et al., 2008). However, not all formulations exhibit DREs, and predicting when they will occur has proved challenging.

A previous work, upon which this paper expounds, has established protocols for quantifying DREs in conversion (α) (Equation 1) and glass transition temperature (T_g) (Equation 2) for a polymer system by determining the change in properties at two different line speeds but at the same total dose (Schissel et al., 2017).

$$\alpha DRE(dose) = \left|\alpha_{6\ m/min} - \alpha_{\ 60\ m/min}\right| \quad (1)$$

$$T_g DRE(dose) = \left|T_{g,6\ m/min} - T_{g,60\ m/min}\right| \quad (2)$$

This previous study compared the DREs of five phenyl acrylate monomers and determined that if a monomer exhibited a large αDRE, that monomer would exhibit a comparably large $T_g DRE$. This similarity between the two DRE results facilitates exploration of a larger library of monomers since no specific monomer structure is required to obtain $T_g DRE$, as is the case with αDRE. Furthermore, DREs were minimized as dose and monomer size increased across the five-monomer series. It was hypothesized that this decrease in DREs for the larger monomers could be attributed to the greater number of labile bonds (primarily abstractable hydrogens) on the molecule, which increases the likelihood of radical formation and chain transfer.

Additionally, recent advancements in calculating the radiation chemical yield, or G-value, of a monomer allow for a more fundamental inquiry into the hypothesized connection between

labile bonds and DREs (Thiher et al., 2019a; Thiher et al., 2019b; Thiher et al., 2020). Specifically of interest in this work is the primary radical radiation chemical yield ($G(R^{\bullet})$), which quantifies the moles of primary radicals formed per Joule of energy absorbed by the system (Makuuchi and Cheng, 2012). Establishing the $G(R^{\bullet})$ value for monomers enables correlation of bond lability to the foundational force behind radical polymerization kinetics – primary radicals. Previously, it was found that monomers with a large number of labile bonds will generally produce more primary radicals (Thiher et al., 2020). However, what is not well established is how radical formation is impacted by dose rate.

Early attempts to determine the relationship between dose rate and radical formation were made by Chapiro in 1962 (Chapiro, 1962). Chapiro compiled $G(M^{\bullet})$ data, which are the G-values of the portion of primary radicals that become initiating radicals, collected at different dose rates for pure methyl methacrylate, styrene, vinyl acetate, and methyl acrylate from various research groups. The G-values of these first two neat monomers were independent of dose rate in certain regimes but dependent on dose rate in others (See Figures 1 and 2 in (Thiher et al., 2019a)). The dose rate data for vinyl acetate and methyl acrylate were less conclusive.

Because these G-values were determined by different researchers, using different types of ionizing radiation (gamma ray, x-ray, and electron beam), and with different pieces of equipment, it is difficult to determine if G-values are truly affected by dose rate from these data alone. No other sources were found by the authors that address this relationship between dose rate and G-values for polymerization reactions. Additionally, the dose rates used to determine the G-values in the studies compiled by Chapiro are ~1,000 times lower than the dose rates used for typical industrial EB polymerizations today. Although Chapiro concluded that there are different dose rate regimes, it is entirely possible that today's typical industrial dose rates simply fall into a regime with different responses than those investigated by Chapiro.

Moreover, Chapiro's compilation of data related the initiating radical radiation chemical yield $G(M^{\bullet})$ to dose rate rather than the primary radical yield $G(R^{\bullet})$. Especially in ionizing radiation polymerization, for which the formation of initiating radicals is only one of several possible secondary reactions (Thiher et al., 2019a; Thiher et al., 2020), determining how dose rate affects primary radical formation is an important cornerstone to establish. The available methods of calculating $G(R^{\bullet})$ also require fewer and more straightforward assumptions than those for calculating $G(M^{\bullet})$ (Thiher et al., 2019a).

Furthermore, these radiation yields could be useful to explore the impact of dose rate on polymerization kinetics. The traditional fundamental kinetic equation for the rate of polymerization (R_p) has a first-order dependence on the initiating radical concentration ($[M^\bullet]$), where $[M]$ is the concentration of monomer and k_p is the propagation rate constant (Equation 3). The first way dose rate could impact $[M^\bullet]$, and thus R_p, is through $G(R^\bullet)$. If $G(R^\bullet)$ is dependent on dose rate, the number of primary radicals produced will change; since primary radicals beget initiating radicals, $[M^\bullet]$ will be affected.

If $G(R^\bullet)$ is *not* a function of dose rate, a second possible relationship may exist between dose rate and $G(M^\bullet)$. For example, at high dose rates, given $G(R^\bullet)$ is constant, the instantaneous concentration of primary radicals will be greater than at low dose rates. This greater value of $[R^\bullet]$ could impact $G(M^\bullet)$: a greater concentration of primary radicals could influence the efficiency of converting primary to initiating radicals, for instance, if primary radical termination becomes more prevalent. In this case, $G(M^\bullet)$ would be dependent on dose rate.

Finally, it is also possible that the reaction could deviate from the traditional relationship between R_p and $[M^\bullet]$, given the right circumstances. Odian reports of one such instance where R_p becomes independent of the initiating radical concentration if the concentration of primary radicals becomes too high (Equation 4) (Odian, 2004). In this example, R_p is instead dependent on two additional rate constants: the initiation rate constant (k_i) and the primary termination rate constant (k_{tp}). As the dose rate increases, the instantaneous radical concentration within a sample should also increase, providing the possibility for R_p to transition away from the classic kinetic definition (Equation 3).

$$R_p = k_p[M^\bullet][M] \tag{3}$$

$$R_p = \frac{k_p k_i[M]^2}{k_{tp}} \tag{4}$$

Starting with a basis in monomer chemistry, exploring the influence dose rate has on radical formation and rate of polymerization will further the understanding of what causes dose rate effects in electron-beam polymerization. In order to assess the validity of the hypothesis that DRE is related to the number of labile bonds, the $T_g DREs$ of several systematically chosen monomers were determined. These additional monomers were selected to complement data from the previous study conducted by Schissel et al. (2017), as well as to further investigate the

importance of bond lability. Dynamic mechanical analysis was used to determine the T_g of samples polymerized at different doses and dose rates, from which data the T_gDREs were calculated. In addition, the primary radical radiation chemical yield for these monomers was quantified at different dose rates to investigate radical formation, which is hypothesized as the fundamental cause for the impact labile bonds have on DREs. Finally, R_p was measured *via* Raman spectroscopy to determine how radical formation at different dose rates affects polymerization kinetics. In turn, this knowledge will inform the chemical structure / processing conditions / polymer property relationships industrial formulators need to increase performance of EB inks, coatings, and adhesives and expand application of EB polymerization to new areas.

2. Experimental

2.1 Materials

Nine acrylate monomers were chosen to investigate the cause and effect of dose rate in this study: dodecyl acrylate (DDA, TCI America); 2-(2-ethoxyethoxy)ethyl acrylate (EEEA, TCI America); phenyl acrylate (PA, MP Biomedical); cyclohexyl acrylate (CHA, TCI America); benzyl acrylate (BA, MP Biomedical); tetrahydrofurfuryl acrylate (THFA, Aldrich); 2-phenylethyl acrylate (PEA, Polysciences); 2-phenoxyethyl acrylate (POEA, TCI America); and 2-hydroxy-3-phenoxypropyl acrylate (HPOPA, Sartomer) (Figure 1).

Monomers PA and BA were a part of the previous study and were initially chosen because the phenyl ring provided a stable bond in Raman spectroscopy measurements for determining polymer conversion (Schissel et al., 2014). CHA and THFA were selected for this study because of their structural similarity to PA and BA, respectively. The major difference between the two monomer pairs is the additional hydrogens for abstraction in the aliphatic ring (in CHA and THFA) compared to the aromatic ring (in PA and BA). The impact of electron-withdrawing groups on ease of hydrogen abstraction was examined using EEEA (ether moieties) and DDA (aliphatic moieties).

Additionally, the remaining monomers from the previous study – PEA, POEA, and HPOPA – were introduced for the R_p comparison. These three monomers, along with PA and BA, create a 5-monomer series across which the number of bonds and/or abstractable hydrogens between the phenyl group and acrylate moiety is systematically increased. The 5-monomer

series was chosen for the R_p comparison because each monomer contains the phenyl ring necessary for accurate Raman measurements.

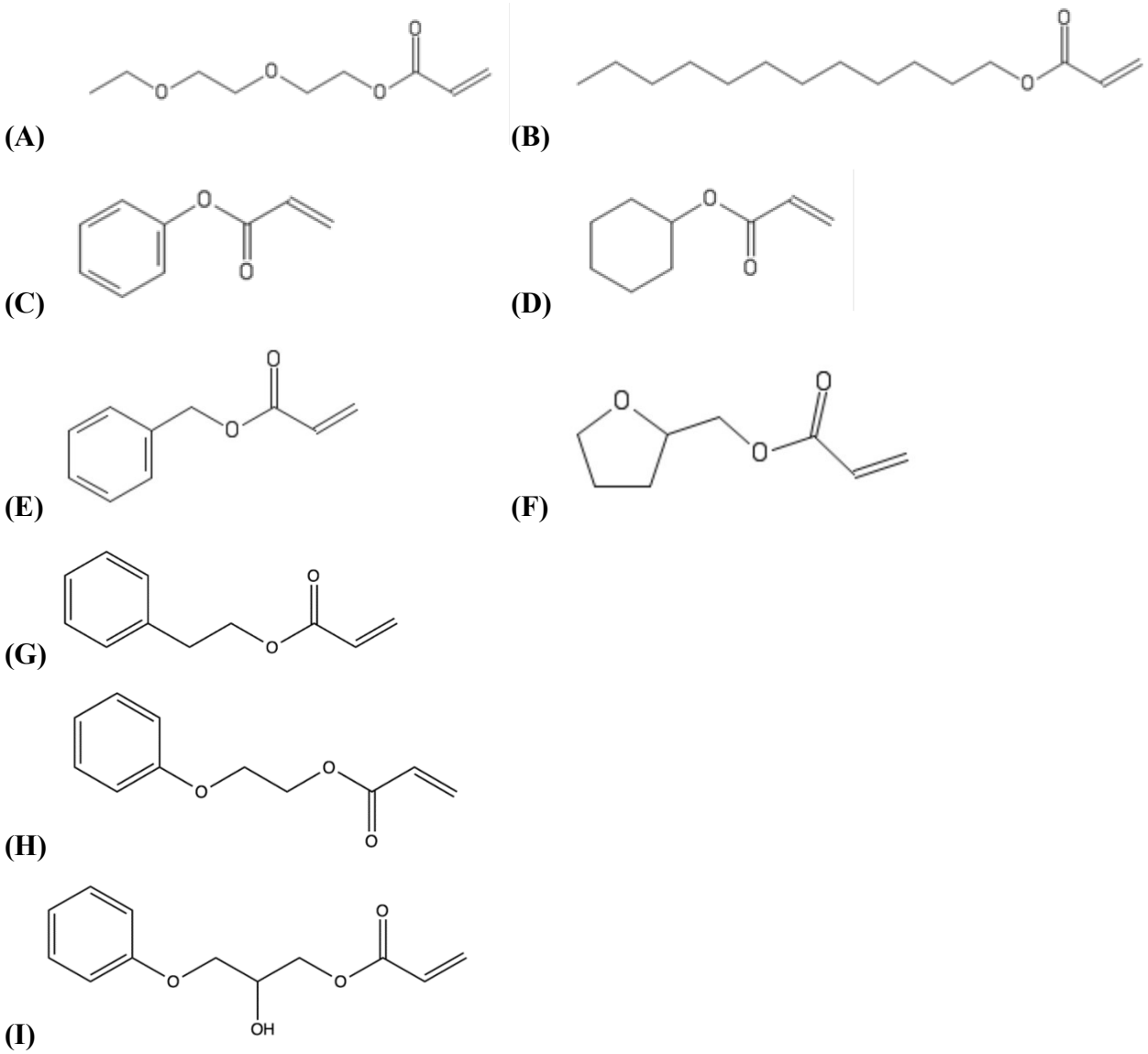

Figure 1. The chemical structures of the acrylate monomers used in this study: (A) EEEA, (B) DDA, (C) PA, (D) CHA, (E) BA, (F) THFA, (G) PEA, (H) POEA, (I) HPOPA. Monomers (A) – (F) were used in studies described in Sections 3.1 and 3.2; monomers (C), (E), and (G) – (I) were used in studies described in Section 3.3.

An aliphatic urethane diacrylate oligomer, Ebecryl 8807 (proprietary structure (for generic structure, see Figure 10 in (Nik Salleh et al., 2009)), Allnex) (Allnex, 2018), was added to each of the monomer formulations used for dynamic mechanical analysis (DMA) to achieve

the necessary film properties for mechanical-property testing (Section 3.1). The free-radical inhibitor 2,2,1-diphenyl-1-picrylhydrazyl (DPPH, TCI America) was used in the protocol to quantify primary radicals (Sections 3.2 and 3.3). All materials were used as received and stored according to recommendations by the manufacturer.

2.2. Methods

2.2.1. Measuring Glass Transition Temperature

2.2.1.1. EB Film Preparation

Each formulation consisted of a 50/50, by weight, mixture of monomer and oligomer. Because of the high viscosity of the oligomer, the formulations were heated to approximately 60°C to allow mixing of the monomer and oligomer. Once heated, formulations were stirred using a drill with a paddle mixer attachment.

Samples for EB curing were prepared by first treating 10 x 8 cm glass slides using two coats of Rain-X® 2-in-1 glass cleaner and rain repellent. Next, two layers of lab tape (total thickness ~180 μm) were placed on either side of the glass to be used as spacers. A large droplet, approximately 1 mL, of a formulation was then placed near the top of the slide, between the pieces of tape, and covered with a piece of silicone-coated, 34-μm thick polyethylene terephthalate (PET). A straight edge was drawn across the PET to form a uniform film underneath.

The samples on the glass slides were polymerized by EB irradiation through the PET film using an EB accelerator equipped with a variable-speed, fiberglass carrier web (BroadBeam EP Series, PCT Ebeam and Integration, LLC). As in previous work (Schissel et al., 2017), three different doses (15, 30, and 60 kGy) and three different line speeds (6, 30, and 60 m/min) were used to cure the films, achieving a range of dose rates from 7 to 300 kGy/s (Table S1). Accelerating voltage and N_2 flow rate were held constant at 250 kV and 0.48 m^3/min, respectively. Beam uniformity was verified using GEX B3 dosimeters (batch DA) (ASTM, 2018). Dosimeters were placed in 2.54 cm increments across a 12.7 cm width. Percent variation was 1.8%. Once polymerized, the clear films were removed from the glass slides and cut into rectangles measuring 6.25 × 25 mm for characterization. The use of silanized (Rain-X®-treated) glass and silicone-coated PET assisted in the release of the polymer film.

2.2.1.2. Dynamic Mechanical Analysis

A dynamic mechanical analyzer (Q800 TA Instruments) equipped with a film tension clamp was used to find the T_g of the polymer films. A mono-frequency strain, temperature ramp sequence was used to collect tan δ values as a function of temperature. Temperature was increased at a rate of 3°C/min over a broad temperature range at a constant oscillating frequency of 1 Hz and a sinusoidal strain of 0.05%. The polymer T_g was taken as the maximum of the tan δ peak (Figure S1). Measurements were repeated in triplicate for these data, and the standard deviation of three averaged T_g values was ± 2.2ºC. The resulting T_g values were used to calculate $T_g DRE$ (Equation 2).

2.2.2. Modeling Hydrogen Abstraction

Spartan Version 6.1 (Wavefunction, Inc.) was used to calculate the energy required to radicalize monomers *via* hydrogen abstraction. Although radicals can form through the cleavage of other bonds during exposure to ionizing radiation, the bond dissociation energy calculations are more complicated and would require significantly more processing time. Furthermore, pulse radiolysis studies of the radical structures created by EB exposure indicate that hydrogen abstraction is one of the most likely methods of radical formation (Knolle and Mehnert, 1995). The energy required to break a bond is dependent on the surrounding bonds; therefore, the energy required to abstract each hydrogen on a monomer (ΔE) was calculated independently using the following equation:

$$\Delta E = (E_{radicalized\ monomer} + E_{abstracted\ hydrogen}) - E_{monomer} \quad (5)$$

The E-values were determined using the ωB97X-D/6-31G* density functional model.

2.2.3. Quantifying Primary Radical Concentration

The methods used to determine primary radical radiation chemical yield ($G(R^{\bullet})$) have been described in detail previously (Thiher et al., 2019b), and only a brief outline of the method is presented here. (Note that the units of the G-value have been updated from radicals per 100 eV (used in early literature) to mol/J (the modern definition) by multiplying by 1.03 x 10^{-7}.) Primary radicals were quantified using the inhibition method (Chapiro, 1962), in which 2 wt% of the

free-radical inhibitor DPPH was added to the formulation of pure monomer. When a DPPH-inhibited formulation is exposed to the EB, primary radicals formed. These primary radicals then react irreversibly with the inhibitor, inducing a color change (Alger, 1996). The disappearance of inhibitor DPPH is directly proportional to the rate of radical formation (R_R) and was measured as a decrease of the peak absorption intensity at 525 nm using UV-Vis spectroscopy (DU-62 Spectrophotometer, Beckman). After determining the rate of radical formation, Equation 6 was used to calculate $G(R^{\bullet})$, since the density (ρ) and dose rate $\left(\frac{dD}{dt}\right)$ were known.

$$G(R^{\bullet}) = \frac{R_R}{\rho \frac{dD}{dt}} \tag{6}$$

Measurements were repeated in triplicate for these data, and the standard deviation of three averaged $G(R^{\bullet})$ values was $\leq \pm 0.05$. R_R was also used to calculate the number of primary radicals formed after a specified time (t):

$$[R^{\bullet}] = R_R \times t \tag{7}$$

The values of both $[R^{\bullet}]$ and $G(R^{\bullet})$ calculated by this indirect method are likely lower than the actual values. This discrepancy is a result of a limitation on the inhibitor method. While it is assumed that the inhibitor reacts with all primary radicals, it cannot account for non-reactive radical species, recombined radicals, or other radical termination reactions. Thus, *apparent* $G(R^{\bullet})$ and $[R^{\bullet}]$ values are calculated, and this concept of apparent values is described in detail in a previous paper (Thiher et al., 2019b).

2.2.4. Measuring Conversion and Rate of Polymerization

2.2.4.1. EB Film Preparation

One hundred µL of each pure monomer formulation was pipetted into aluminum weigh dishes with an 11 mm diameter. The aluminum weigh dishes were secured to Q-panels for easy transport and EB exposure. EB polymerization of the films followed the procedure in Section 2.2.1.1. with the exception of the doses and line speeds. Once prepared, the samples were polymerized at the dose and line speed combinations listed in Table 1 to create a kinetic profile *vs.* time. Line speed was altered to maintain a consistent dose rate of 30 kGy/s. For each dose/line speed combination, a unique sample was used (*i.e.*, no sample was exposed to the beam

more than once) to ensure no pulsed ebeam effects confounded the data (Richter, 2007). Increasing the dose rate to 300 kGy/s was achieved by increasing the line speed 10x.

Table 1. Dose and line speed combinations used to create kinetic profiles for conversion and rate of polymerization experiments at 30 kGy/s.

Dose (kGy)	132	150	165	183	206
Line speed (m/min)	3.8	3.4	3	2.7	2.4

2.2.4.2. Raman Microscopy

Raman microscopy was used to determine conversion of the 5-monomer series samples after EB exposure. In order to eliminate error from instrumental variation and EB bombardment, a reference peak was used. Previous work has established the reaction peak at 1636 cm^{-1} (indicative of the -C=C- bond in the acrylate moiety) and a reference peak at 1613 cm^{-1} (indicative of the -C=C- bonds in the phenyl ring) (Schissel et al., 2014). Fractional conversion, α, was calculated using the following equation:

$$\alpha = \left(1 - \frac{I_{rxn}(P)/I_{ref}(P)}{I_{rxn}(M)/I_{ref}(M)}\right) \quad (8)$$

where $I_{rxn}(P)$ and $I_{ref}(P)$ are the peak intensities of the reaction and reference peak of the polymer, respectively; $I_{rxn}(M)$and $I_{ref}(M)$ are the peak intensities of the reaction and reference peak of the monomer (Schissel et al., 2014).

EB-exposed samples were transferred to aluminum Q-panels for analysis. Raman spectra of the samples were collected using an optical microscope (DMLP Leica) connected to a modular research Raman spectrograph (HoloLab 5000R, Kaiser Optical Systems, Inc.) *via* a 100-μm collection fiber. A single-mode excitation fiber carried an incident beam of 785-nm near-infrared laser to the sample through a 10x objective with a numerical aperture of 0.25 and a working distance of 5.8 mm. Laser power at the samples was ~8 mW. Spectra were collected with an exposure time of 30 seconds and 3 accumulations. Ten monomer spectra were collected and averaged to provide accurate values for $I_{rxn}(M)$ and $I_{ref}(M)$ to use in Equation 8. The error in the conversion measurements due to instrumental variation is expected to be ±0.05.

Using the conversion data calculated from Raman spectra, the instantaneous monomer concentration, $[M]$, was calculated as follows:

$$[M] = [M]_0(1 - \alpha(t)) \quad (9)$$

where the initial monomer concentration, $[M]_0$, is simply the density (in g/L) multiplied by the molar mass (in mol/g), since the formulation was pure monomer. Thereafter, $[M]$ was plotted as a function of time and fitted to a straight line, with goodness of fit (as measured by R^2 values) greater than 0.8. By definition (Odian, 2004), the rate of polymerization is the negative slope of this line: $R_p = -\frac{d[M]}{dt}$.

3. Results and Discussion

This study aimed to investigate how changes in radical concentration, brought on by altering monomer chemistry and dose rate during EB polymerization, impacted DREs. The DREs of monomers with differing numbers of labile bonds were quantified by determining polymer T_g, which was measured by DMA. Radical formation was quantified by measuring monomer G-values. Rate of polymerization was calculated using Raman spectroscopy. Differences in radical formation and R_p were observed and correlated to DREs.

3.1. Confirmation of DRE Trends with Expanded Monomer/Oligomer Series

Previous work has established that monomers with a limited number of labile bonds experience large dose rate effects, whereas monomers with more labile bonds experience little to no DREs. In addition, these DREs were correlated to conversion and T_g (Schissel et al., 2017). Three pairs of monomers (mixed 50/50 with oligomer, Figure 1) were selected to confirm and expand on this research by evaluating their T_g and $T_g DRE$ values. In choosing to focus on $T_g DRE$ values, a wider selection of monomers was available for evaluation. Both dose and line speed were systematically varied in order to understand the impact of dose on dose rate effects.

As a general trend, the T_g of the polymers studied remains the same or increases with increasing dose at a constant line speed (Table 2). Exceptions to this trend are attributed to the values being within the standard deviation of the instrument. This result is consistent with

previous work and is ascribed to increases in conversion (Schissel et al., 2017) and crosslinking, when applicable (Sperling, 2001). With an increase in initiating energy (dose), it follows *via* traditional kinetics that conversion also increases (Odian, 2004). Conversion and T_g are well known to be correlated: at low conversions, the threshold molecular weight needed to reach a polymer's maximum T_g may have not yet been reached, and the remaining monomer may also suppress the T_g by plasticizing the film (Odian, 2004). Thus, films polymerized with higher doses should have higher conversions and T_g values. Conversion measurements were not included in these studies because not all monomers contained an EB-radiation stable bond, which is needed for accurate Raman measurements (Schissel et al., 2014).

Table 2. Comparison of T_g values (ºC) for six acrylate monomers (mixed 50/50 with oligomer) at three different doses and line speeds. DMA was used to collect T_g data. (*Film weakness prevented data collection for DDA at 15 kGy, 60 m/min.)

	6 m/min			30 m/min			60 m/min		
	15 kGy	**30 kGy**	**60 kGy**	**15 kGy**	**30 kGy**	**60 kGy**	**15 kGy**	**30 kGy**	**60 kGy**
PA	26	49	57	3	31	50	-21	6	19
CHA	53	52	55	47	49	52	40	49	51
BA	21	24	27	-3	2	14	-26	-19	14
THFA	11	23	23	12	23	21	15	20	22
EEEA	-5	-8	-9	-7	-8	-9	-9	-7	-8
DDA	4	4	4	-3	-4	2	*	-6	-5

To confirm DREs are affected by the lability of the bonds within a monomer, Equation 2 was used to calculate the $T_g DRE$ from Table 2 data for the studied monomer formulations (Figures 2 and 3). PA and CHA are identical monomers, save for the conjugation of the aromatic ring. Because of this conjugation, PA not only has fewer hydrogens than CHA, but the hydrogens on the phenyl ring are also less prone to abstraction because of the stabilizing effects of resonance. Comparison of the T_g data for PA and CHA shows that the greater number of abstractable hydrogens on the cyclohexyl moiety of CHA significantly lessens the magnitude of the $T_g DRE$ for all dose and line speed combinations (Figure 2). At 60 kGy, for example, the $T_g DRE$ is reduced by 34ºC between the two formulations. Despite having a lower

magnitude T_gDRE than PA, CHA follows the established trend of having its largest T_gDRE at 15 kGy (Schissel et al., 2017).

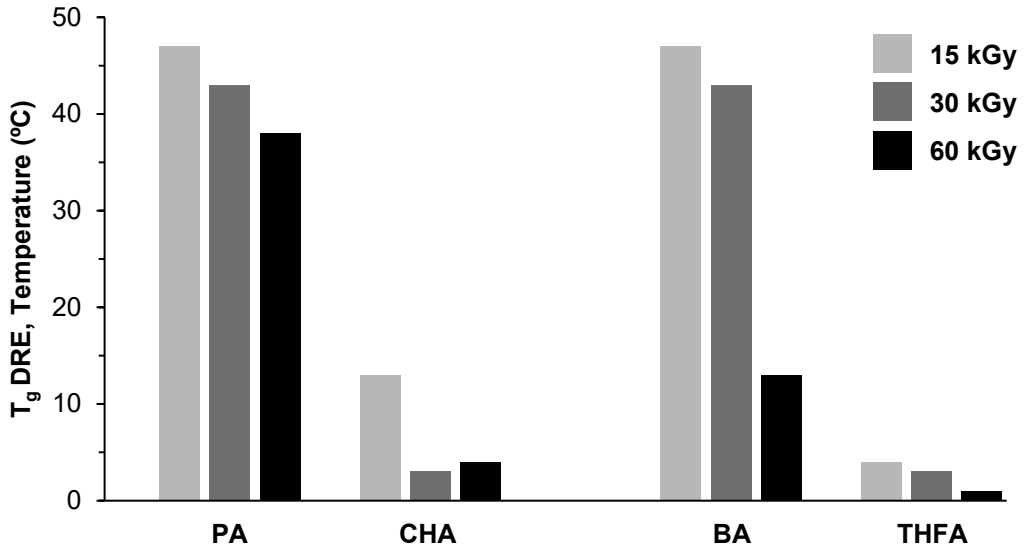

Figure 2. The glass transition temperature DREs, at three different doses, for two pairs of monomer/oligomer formulations: (1) PA and CHA and (2) BA and THFA. The larger number of abstractable hydrogens on CHA and THFA decreases the DRE in comparison to PA and BA, respectively.

Similarly, a comparison of the BA and THFA T_gDREs shows that THFA, with a greater number of abstractable hydrogens, has a lower DRE than BA (Figure 2). BA has a ≥ 40ºC difference in T_gDRE magnitude over THFA at both 15 and 30 kGy. Furthermore, just like PA and CHA, the T_gDREs of BA and THFA decrease as the total dose increases.

These comparisons of PA/CHA and BA/THFA not only continue to support the hypothesis that the presence of labile bonds on a monomer reduces DREs, but also work to eliminate monomer size as a valid argument for affecting DREs. In previous work with the five-monomer series, both the size of the monomer molecule and the number of labile bonds increased with increasing monomer size (Schissel et al., 2017). In this study, these two pairs of monomers were selected to be of similar size to facilitate a focused validation of the abstractable hydrogen theory. Table 3 lists the molecular weight (MW) and molar volume of the monomers

to demonstrate their similarity. The molecular weight and molar volume of PA are 96% and 87%, respectively, of that for CHA. For the BA/THFA pair, THFA is actually slightly smaller than BA although it has more abstractable hydrogens: THFA is 96% of the weight of BA and 93% of the molar volume. Relating the monomer size and T_gDRE data shows no correlation between the two properties (Figure 2).

Table 3. Property comparisons for the PA/CHA and BA/THFA monomer pairs. Molar volume was calculated using the density (at 20ºC) provided by the manufacturer.

	Formula	MW (g/mol)	Molar Volume (cm^3/mol)
PA	$C_9H_8O_2$	148.16	137.4
CHA	$C_9H_{14}O_2$	154.21	157.5
BA	$C_{10}H_{10}O_2$	162.19	153.3
THFA	$C_8H_{12}O_3$	156.20	142.9

Comparison of T_gDRE data for DDA and EEEA indicates not only is the number of abstractable hydrogens in a monomer important, but the bond strength of the hydrogens also influences DREs (Figure 3, note the change in y-axis magnitude compared to the previous figure). Setting aside the hydrogens within the acrylate moiety (which both monomers have in common), DDA contains 25 hydrogens while EEEA only contains 13 hydrogens (Figure 1); however, the T_gDRE for EEEA is smaller than that of DDA.

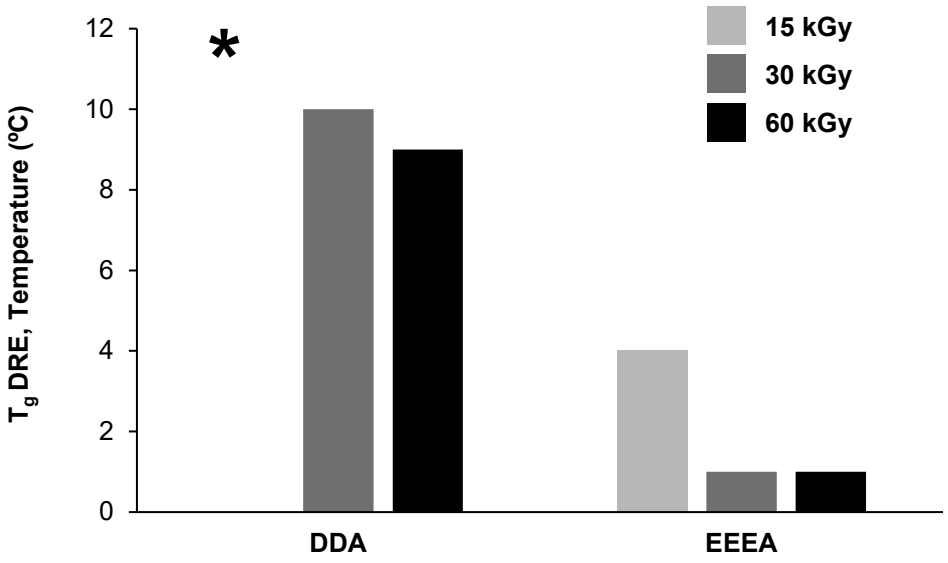

Figure 3. The glass transition temperature DREs, at three different doses, for the DDA and EEEA monomer/oligomer formulations. The more easily abstractable hydrogens in the backbone of EEEA decreases the DRE. (*Film weakness prevented data collection for DDA at 15 kGy, 60 m/min.)

The lower $T_g DRE$ in EEEA can be attributed to the oxygens within the backbone. The oxygens are strong electron-withdrawing groups, which weaken the surrounding C-H bonds. Therefore, the hydrogens near the oxygen of EEEA are likely more easily abstracted compared to those on DDA. The bond dissociation energy, ΔE in Equation 5, was modeled using Spartan to demonstrate this effect (Table 4).

Table 4. Energy required to break C-H bonds on DDA and EEEA modeled using Spartan software. The oxygens in the backbone of EEEA reduce the energy requirement for the abstraction of the adjacent hydrogen.

Monomer	Bond	Dissociation Energy x 10^{19} (J)
DDA	CH_3CH_2C – **H_2**	5.58
EEEA	CH_3CH_2CO – **H_2**	4.87

Although the bond energy is only reduced by approximately 0.71 x 10^{-19} J in oxygen-adjacent C-H bonds, EEEA is able to achieve almost no $T_g DRE$ (1ºC) at 30 and 60 kGy, while DDA has a ~10ºC $T_g DRE$ at the same energies with twice as many abstractable hydrogens

available. The lower bond dissociation energy not only increases the probability that an accelerated electron will have sufficient energy to break the bond, but it also saves energy to be used on other bonds.

3.2. Radiation Chemical Yield Studies with Expanded Monomer Series

Results from Section 3.1 provide evidence that the quantity and strength of labile bonds have a strong impact on the DRE magnitude of a monomer. To explore this relationship between bond lability and DRE magnitude more directly, the focus of this study was turned to primary radical formation. During EB exposure, primary radicals are formed through the cleavage of bonds (Chapiro, 1962; Makuuchi and Cheng, 2012; Richter, 2007). It is expected that monomers with a large number of labile bonds will produce more radicals (Thiher et al., 2020), but little research has been devoted to understanding how dose rate will impact radical formation (Chapiro, 1962). As discussed in Section 1, an increase in primary radical concentration ($[R^{\bullet}]$) may have an impact on polymerization rate (R_p) by affecting the initiating radical concentration ($[M^{\bullet}]$).

Thus, primary radical formation was quantified for each pure monomer by measuring the primary radical radiation chemical yield $G(R^{\bullet})$ at two different dose rates (Figure 4). The dose rates chosen for this experiment (30 kGy/s and 300 kGy/s) fall within the range of the dose rates used to measure DREs in Section 3.1 (7 kGy/s to 300 kGy/s). At both dose rates, the total dose delivered was identical (~200 kGy).

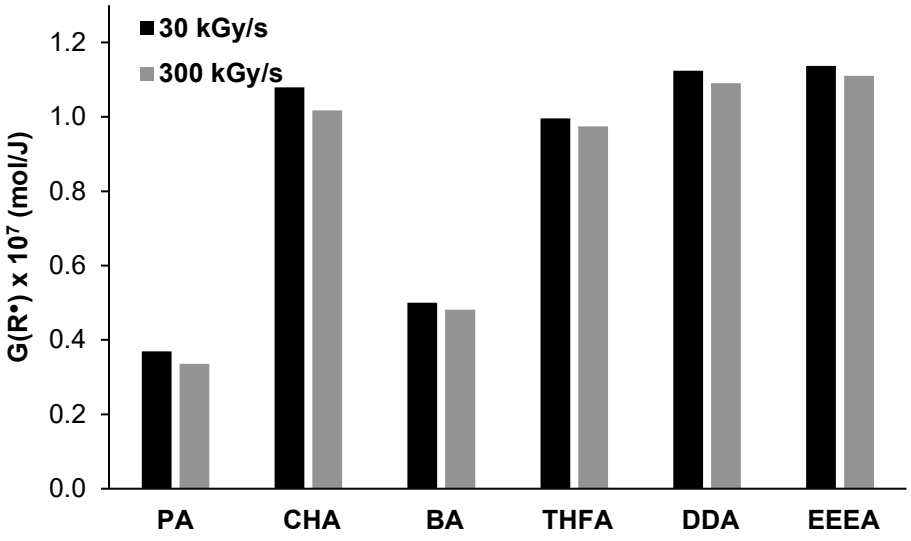

Figure 4. The values of $G(R^{\bullet})$, collected for pure monomers, are dependent on monomer chemistry but are independent of dose rate.

The value of $G(R^{\bullet})$ was expected to increase with an increase in labile bonds, yet perhaps unsurprisingly this expected result was found to be an oversimplification of the true trend. In comparison of the pairs PA/CHA and BA/THFA, the monomers with the unconjugated rings (and thus more labile bonds) do indeed produce more primary radicals. However, there is little difference in the values of $G(R^{\bullet})$ for the DDA/EEEA pair despite a difference in the number of labile hydrogens, suggesting that, as with DREs, the dissociation energy of the labile bonds is also an important factor. In fact, the $G(R^{\bullet})$ results in Figure 4 correlate quite well with the DRE results in Figures 2 and 3: PA and BA have large DREs and relatively low $G(R^{\bullet})$ values, while the other four monomers have small DREs and relatively high $G(R^{\bullet})$ values.

For all six monomers, changing the dose rate resulted in only minute changes to $G(R^{\bullet})$, within error of the measurement. There was no difference in the results for monomers exhibiting large dose rate effects (*i.e.*, PA and BA) versus those exhibiting little to no dose rate effects. The value of $G(R^{\bullet})$ is a measure of the number of radicals formed per unit dose (McNair, 1981). Because both the slow and fast dose rate experiments used the same total dose, isolating dose rate as a variable, it is therefore concluded that values of $G(R^{\bullet})$ are independent of dose rate for the studied dose rate range. Unlike the dose rate regimes Chapiro found when studying $G(M^{\bullet})$ (Chapiro, 1962), it is expected that further testing will conclude $G(R^{\bullet})$ is wholly independent of dose rate, until such extreme doses are reached that the available energy exceeds the required amount to break all present labile bonds.

Since the total number of primary radicals formed during the slow and fast dose rate reactions is the same, it follows that the instantaneous radical concentration must be higher for the fast dose rate reaction because of its shorter duration. The fast dose rate exposure happens 10 times faster than the slow dose rate exposure; consequently, the instantaneous radical concentration should be 10 times higher for the duration of the fast dose rate exposure time, making the classic steady-state assumption (Figure 5A). Calculating the radical concentration after 0.1 s of EB exposure shows exactly that – a 10-fold increase in dose rate results in a ~10-fold increase in radical concentration for all 6 monomers (Figure 5B).

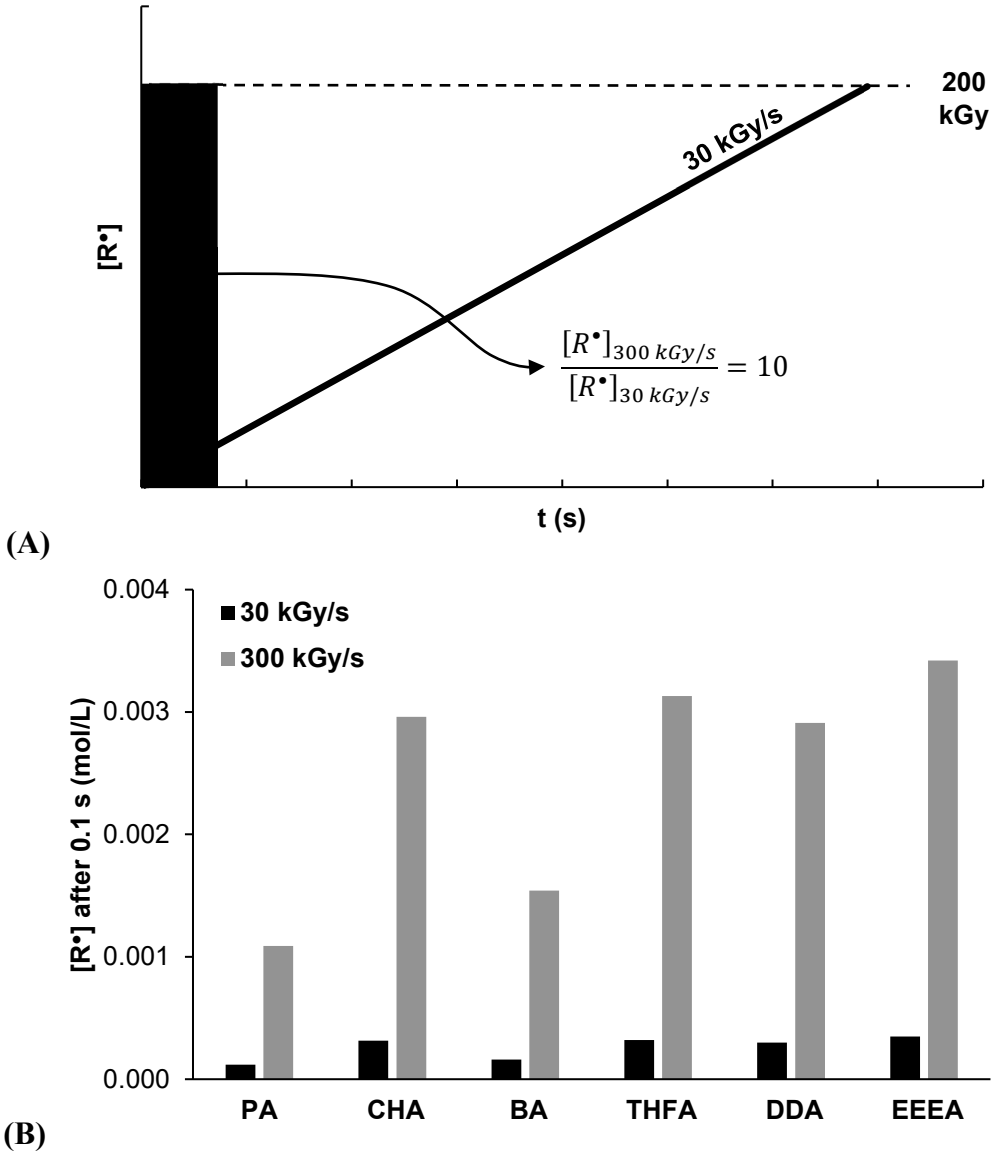

Figure 5. (A) Theoretical illustration of the effects of dose rate on the instantaneous $[R^{\bullet}]$. While both dose rates achieve the same final $[R^{\bullet}]$ when exposed to the same dose, for the duration of the fast dose rate (300 kGy/s) reaction, the instantaneous $[R^{\bullet}]$ is 10x that for the slow dose rate (300 kGy/s) reaction. (B) The difference in radical concentration at 0.1 s for each pure monomer during the slow and fast dose rate exposures. Increasing the dose rate 10-fold increases the instantaneous radical concentration nearly 10-fold.

Thus far, it has been established that dose rate does not affect $G(R^{\bullet})$ (Figure 4), and the theoretical relationship of Equation 6 (Figure 5) has been confirmed. Assuming k_p is relatively constant (see Section S3), it can be concluded that dose rate effects must, therefore, be caused by

a non-reciprocity later in the kinetic mechanism. As presented in Section 1, the next relationship to consider is that of dose rate and $G(M^{\bullet})$. However, determining if $G(M^{\bullet})$ is dependent on dose rate is not straightforward. Current methods of calculating $G(M^{\bullet})$ rely on assumptions concerning the ratio of radicals to polymer chains and the method of termination (see Section 3.2.1. Conversion Method in Thiher et al. (2019a)) or assume photopolymerization rate constants are valid for EB polymerization reactions (see Section 3.2.2. Kinetic Method in Thiher et al. (2019a)). While both methods can provide useful information in other contexts, the assumptions they require leave too much ambiguity surrounding the relationship between $G(M^{\bullet})$ and dose rate effects to be of use. For instance, in addition to using photopolymerization kinetic constants, the Kinetic Method also relies on the assumption that R_p is defined as in Equation 3 (Thiher et al., 2019a), which, as discussed in Section 1, may not be a relevant assumption for all dose rates. Without a more straightforward method to measure $G(M^{\bullet})$, it may be impossible to separate which factor is causing dose rate effects: a change in $G(M^{\bullet})$ or a change in the definition of R_p. Thus, the choice was made to pull back the focus and more broadly investigate R_p, a variable that can be measured empirically.

3.3. Polymerization Rate Studies with 5-monomer Series

To investigate the impact of R_p on dose rate effects in EB polymerization, the 5-monomer series used in previous experiments was revisited (Figure 1) (Schissel et al., 2017). This selection was made since some monomers in the expanded monomer series do not contain the phenyl ring necessary to perform accurate conversion measurements, which are needed to calculate R_p. However, the 5-monomer series of phenyl acrylate monomers exhibits a range of DREs and was previously used to compare conversion DREs and polymerization rates. Note, data from this previous study used the 5-monomer series in a monomer/oligomer formulation. The data presented here are for pure monomers.

Before investigating the impact of dose rate on R_p, the values of $G(R^{\bullet})$ and $[R^{\bullet}]$ after 0.1 s were calculated for the 5-monomer series at 30 kGy/s and 300 kGy/s (Figure 6) to confirm the trends seen in the expanded monomer series (Figures 4 and 5). As expected, increasing the dose rate 10-fold had little effect on the values of $G(R^{\bullet})$ for all the monomers in the 5-monomer series (Figure 6A). Furthermore, just as observed for the expanded monomer series, increasing the dose

rate 10-fold resulted in a ~10-fold increase in radical concentration after 0.1 s of EB exposure (Figure 6B).

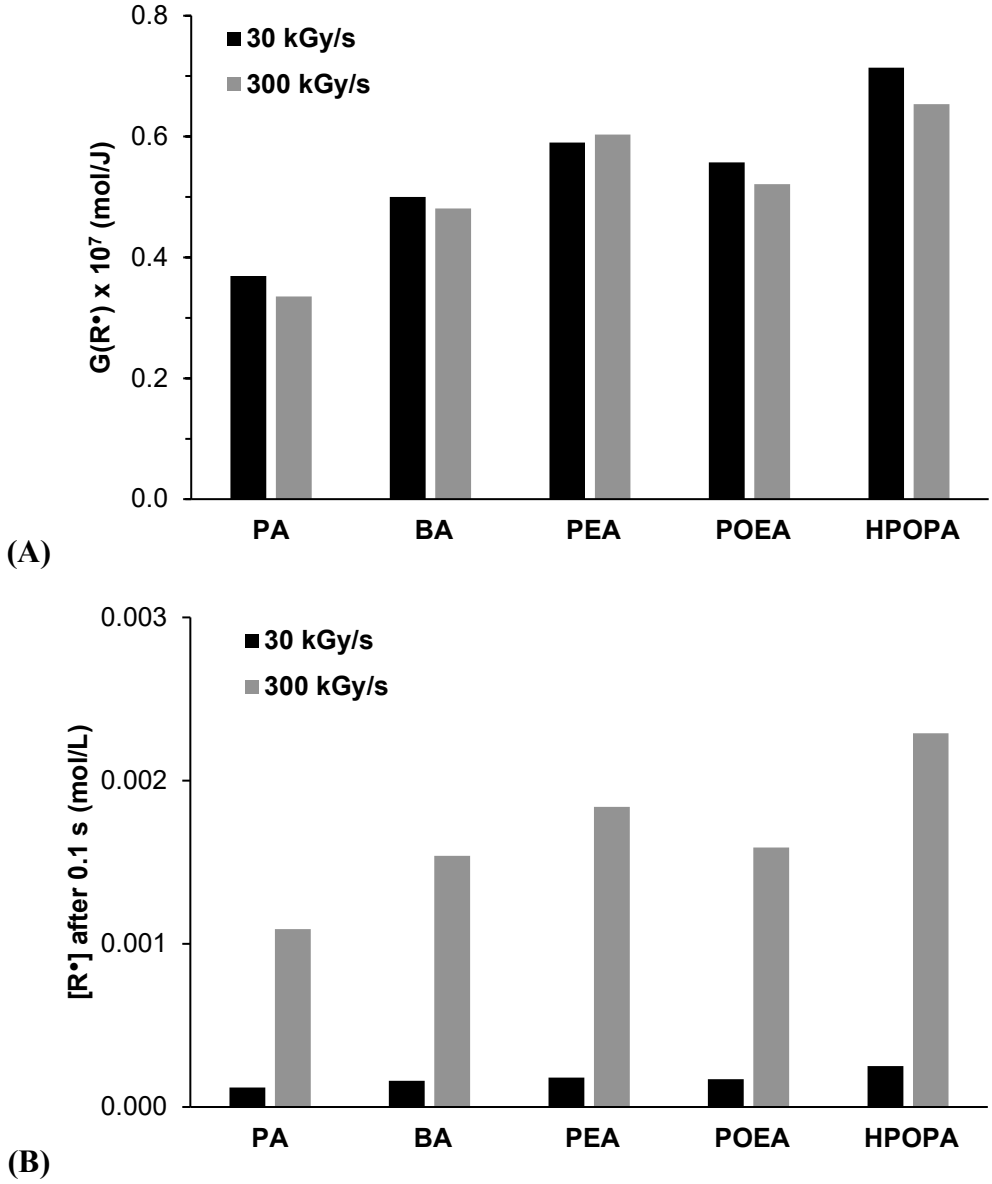

Figure 6. Confirmation of the trends seen in Figures 4 and 5 for pure monomers of the 5-monomer series. (A) The values of $G(R^{\bullet})$ are dependent on monomer chemistry but are independent of dose rate. (B) Increasing the dose rate 10-fold increases the instantaneous radical concentration nearly 10-fold.

Additionally, these data continue to support the hypothesis that increasing the number of labile bonds on a monomer molecule generally increases the ability of the monomer to generate primary radicals upon EB exposure. This trend, shown previously with the PA/CHA and BA/THFA pairs (Figure 5), is clearly evident across the 5-monomers series. POEA is the one

exception to the trend, possibly because of the impact of the oxygen on the bond strength of the surrounding C-H bonds (Thiher et al., 2020).

Next, the 5-monomer series was EB polymerized at dose rates of 30 kGy/s and 300 kGy/s to produce the conversion data for calculating R_p and to establish the magnitude of the dose rate effects. While the 5-monomer series has been studied previously, data have not previously been collected for the pure monomers at these combinations of dose and dose rate. Ultimate conversion of each monomer after the ~200 kGy exposure is reported for each dose rate in Figure 7. Increasing the dose rate from 30 kGy/s to 300 kGy/s decreased the conversion of PA by a factor of 5, even though the total dose delivered was identical in both experiments. In contrast, changing the dose rate did not have an impact on the ultimate conversion of HPOPA. The impact of dose rate on the other 3 monomers in the series falls between these two extremes. From Figure 7, it can be concluded that the conversion of HPOPA is independent of dose rate (for the studied range), while the remaining four monomers are dependent on dose rate to varying degrees.

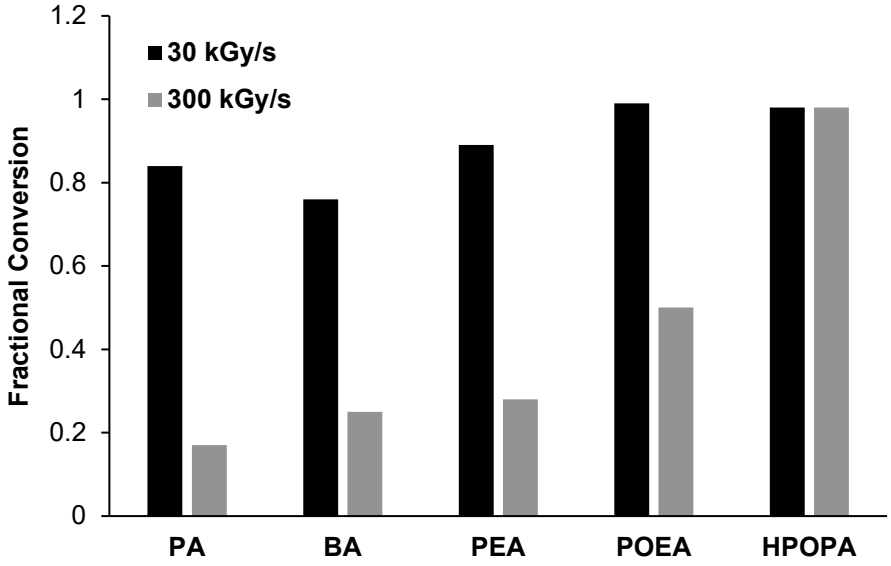

Figure 7. Ultimate conversion of the 5-monomer series (pure monomer) EB polymerized with a total dose of ~200 kGy and dose rates of 30 kGy/s and 300 kGy/s. In contrast to the other monomers, HPOPA, as the monomer with the most labile bonds (Figure 1), shows no change in conversion between the two dose rates.

Conversion data were also used to generate plots of monomer concentration as a function of time, the slope of which is equivalent to the rate of polymerization, R_p (Figure 8 and Table 5).

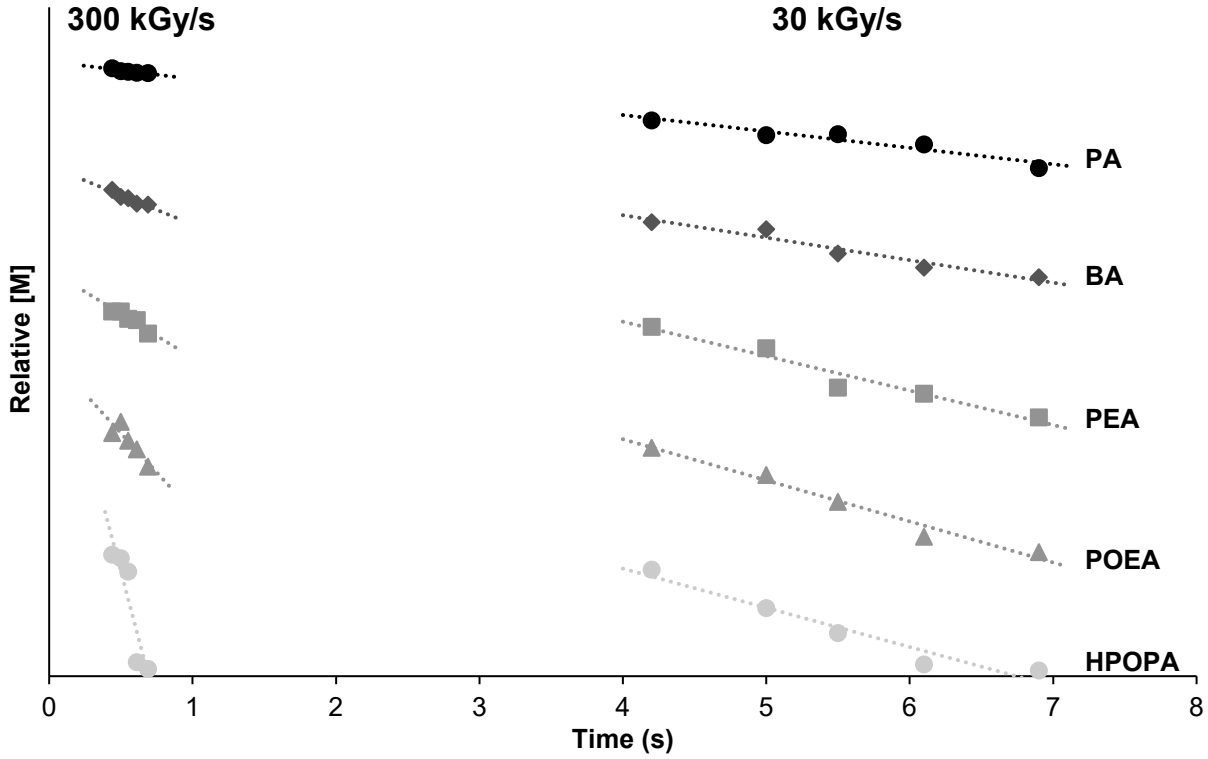

Figure 8. Relative monomer disappearance for the five-monomer series (pure monomer) during EB exposure at dose rates of 30 kGy/s and 300 kGy/s. The rate of polymerization of PA is independent of dose rate, while the rate of polymerization of HPOPA follows classical kinetics and increases 10-fold as the dose rate increases 10-fold. BA, PEA, and POEA fall in between these two extremes.

Table 5. Rate of polymerization for the 5-monomer series (pure monomer) during EB exposure at dose rates of 30 kGy/s and 300 kGy/s.

	$R_{p,30\ kGy/s}$ (mol/L s)	$R_{p,300\ kGy/s}$ (mol/L s)	$\frac{R_{p,300\ kGy/s}}{R_{p,30\ kGy/s}}$
PA	0.76±0.06	0.81±0.04	1.11
BA	1.03±0.04	2.69±0.03	2.61
PEA	1.46±0.05	3.75±0.04	2.57
POEA	1.33±0.05	5.10±0.06	3.83
HPOPA	0.95±0.03	10.33±0.05	10.8

According to classical polymerization kinetics (Equation 3), a 10-fold increase in the propagating radical concentration should result in a 10-fold increase in rate of propagation (R_p). HPOPA, which exhibited no conversion DRE (Figure 7), follows classical kinetics. The ~10-fold increase in radical concentration (Figure 6B) resulted in an $R_{p,300\ kGy/s}/R_{p,30\ kGy/s}$ ratio of 10.8

(Table 5). Visually, there is a distinct difference between the slope of HPOPA disappearance at 300 kGy/s (Figure 8, left) and that at 30 kGy/s (right). Figure 8 illustrates how this distinction between the slopes associated with the two dose rates is eroded with each successively smaller monomer until, with PA, the two dose rates could be graphed on the same line. Numerically, this similarity results in an $R_{p,300\ kGy/s}/R_{p,30\ kGy/s}$ ratio of 1.11 for PA.

While the root cause for the change in R_p – a change in $[M^{\bullet}]$ or a deviation of R_p from classical kinetics – remains to be determined, this kinetic change experienced by PA, BA, PEA, and POEA between dose rates does explain why these four monomers manifest αDREs. In fact, the closer the ratio of $R_{p,300\ kGy/s}/R_{p,30\ kGy/s}$ gets to the expected value of 10, the smaller the DREs become (Figure 9).

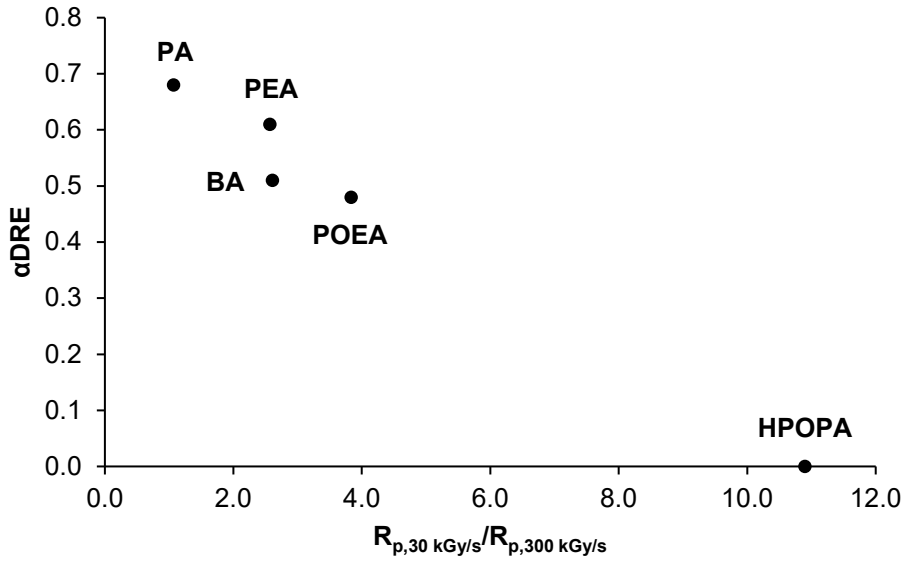

Figure 9. Comparison of αDREs to the $R_{p,300\ kGy/s}/R_{p,30\ kGy/s}$ ratios for the 5-monomer series. HPOPA, a monomer with no measurable DRE, is the only monomer of the series to reach the expected ratio of 10; monomers with αDREs all fall short.

Anything less than a proportional increase in R_p to the reduction in reaction time (*e.g.*, 10 R_p to 1/10 t) results in simply not enough time to reach the same level of conversion. And, as previously stated, changing the conversion of a system can impact other properties, including T_g (Schissel et al., 2017). Thus, other dose rate effects, such as $T_g DRE$s, can be attributed to this change in R_p as well.

The change in R_p alone, however, does not predict the level of conversion at different dose rates. For example, with an $R_{p,300\ kGy/s}/R_{p,30\ kGy/s}$ ratio of 1.11, PA's $R_{p,300\ kGy/s}$ is approximately one tenth of what is expected. Therefore, it follows that the conversion level of PA at 300 kGy/s should be one tenth that of the conversion level at 30 kGy/s, but that is not the case. At a dose rate of 30 kGy/s and dose of 200 kGy, PA achieves a fractional conversion of 0.84, while at 300 kGy/s the fractional conversion achieved is 0.17 or 20% that of the slower dose rate (Figure 7). PA achieved double the conversion at 300 kGy/s than is predicted by its performance at 30 kGy/s and $R_{p,300\ kGy/s}$, suggesting that the change in R_p is not the sole factor in determining the magnitude of DREs. Similarly, BA, PEA, and POEA all performed better than the change in their R_p predict, albeit the deviations were not as great as that for PA.

4. Conclusions

Monomer chemistry plays an important role in the magnitude of DREs experienced during EB polymerization. This work confirms monomer structure trends found in past studies, namely that increasing the number of abstractable hydrogens on a monomer molecule reduced DREs. Additionally, it was demonstrated that monomer size does not correlate with the magnitude of a monomer's DRE, confirming that, while size and quantity of labile bonds typically correlate, it is labile bonds that influence DREs. Furthermore, this work concludes that the bond energy of the available labile bonds is also an important factor.

In addition to confirming and broadening the scope of previous conclusions, this work also established correlations between monomer chemistry, DREs, and some of the most fundamental kinetic components of radical polymerization: the primary radical radiation yield, $G(R^{\bullet})$, and the rate of polymerization, R_p. By determining the $G(R^{\bullet})$ values for the studied monomer series, it was shown that monomers with less labile bonds do indeed produce less radicals than those monomers similarly structured but with more labile bonds, more firmly cementing the connection between bond lability and kinetics. Moreover, values of $G(R^{\bullet})$ were demonstrated to be dependent on monomer chemistry but independent of dose rate for the studied range, and increasing the dose rate 10-fold increases the instantaneous radical concentration ~10-fold. With these results, it can be concluded that DREs do not stem from changes to $G(R^{\bullet})$.

Studying the relationship of R_p and DREs resulted in a clear trend: when R_p fails to increase proportionally with an increase in dose rate, DREs manifest. Further, the greater the disproportionality between R_p and dose rate, the larger the magnitude of αDREs for a monomer. At present, whether the change experienced in R_p over a range of dose rates is due to a change in $[M^{\bullet}]$ or a deviation of R_p from classical kinetics cannot be known using currently available analytical methods. Thus, future work in this arena requires the development of methods to determine $G(M^{\bullet})$ on that rely on kinetic constants from EB-initiated polymerization. Future work should also explore what other factors may influence DREs in addition to R_p, as it was shown with conversion outcomes in this study that R_p is likely not the only factor at play.

Correlating monomer chemistry, radiation chemical yields, and DREs will aid in the development of structure/processing conditions/properties relationships that are currently lacking for EB polymerization. Developing these relationships will not only further the fundamental understanding of EB polymerization – and potentially other types of ionizing radiation polymerization – but will increase the industrial relevance of the technology. Through these relationships, accurate predictions can be made to help identify formulations with polymer properties not currently realized, expanding EB polymerization into new markets. Understanding how monomer chemistry impacts the rate of polymerization, and ultimately DREs, will also prevent unforeseen property changes in the scale-up process, saving time and money.

5. Acknowledgements

This material is based upon work supported by the National Science Foundation under Grant No. 1264622 and The University of Iowa Mathematical & Physical Sciences Funding Program. The authors would also like to acknowledge Dr. Stephen Lapin for his insights and recommendations in the early stages of this project and Kyle McCarthy and Renae Kurpius for their contributions with data collection.

6. References

Allnex, 2018. Ebecryl® 8807. https://allnex.com/en/product/cee3a618-267f-489f-8184-ddb4ec7ff56f/ebecryl-8807 (accessed 22 July 2021).

ASTM, 2018. Standard Practice for Use of a Radiochromic Film Dosimetry System. https://compass.astm.org/EDIT/html_annot.cgi?ISOASTM51275+13 (accessed 22 July 2021).

Alger, M., 1997. Polymer Science Dictionary, third ed. Chapman and Hall USA: New York, pp. 152.

Chapiro, A., 1962. Radiation Polymerization of Pure Monomers in the Homogeneous Liquid Phase, in: Radiation Chemistry of Polymeric Systems. John Wiley & Sons, Inc.: New York, pp. 159-203. https://doi.org/10.1002/pol.1963.100010646.

Cohen, G., 2012. UV/EB Market Trends. RadTech Rep. 26(2), 44-48.

Kinstle, J.F., 1990. Electron-Beam Curing of Polymeric Materials, in: Hoyle, C.E., Kinstle, J.F. (Eds.), Radiation Curing of Polymeric Materials. American Chemical Society: Washington DC, pp. 17-23. https://doi.org/10.1021/bk-1990-0417.ch002.

Knolle, W., Mehnert, R., 1995. On the mechanism of the electron-initiated curing of acrylates. Rad. Phys. Chem. 46(4-6), 963-974. https://doi.org/10.1016/0969-806X(95)00302-E.

Makuuchi, K., Cheng, S., 2012. Radiation processing of polymer materials and its industrial applications. John Wiley & Sons, Inc.: New Jersey. https://doi.org/10.1002/9781118162798.

McNair, A., 1981. ICRU Report 33 - Radiation Quantities and Units Pub: International Commission on Radiation Units and Measurements, Washington DC USA issued 15 April 1980, pp. 25. Journal of Labelled Compounds and Radiopharmaceuticals. 18(9), 1398-1398. https://doi.org/10.1002/jlcr.2580180918.

Nik Salleh, N.G., Yhaya, M.F., Hassan, A., Bakar, A.A., Mokhtar, M., 2009. Development of scratch-and abrasion-resistant coating materials based on nanoparticles, cured by radiation. Internatl. J. Polym. Mater. Vol 58, 422-451. https://doi.org/10.1080/00914030902936501

Odian, G., 2004. Radical Chain Polymerization, in: Principles of Polymerization, fourth ed. John Wiley & Sons, Inc.: New Jersey, pp. 198-349. https://doi.org/10.1002/047147875X.

Rangwalla, I. J., Nablo, S.V., 1990. A Parametric Study of the Electron Curing of Inks and Coatings. Proc. RadTech '90. Vol 1, 18-28.

Richter, K.B., 2007. Pulsed Electron Beam Curing of Polymer Coatings. Proquest: Michigan.

Schissel, S.M., Lapin, S.C., Jessop, J.L.P., 2014. Internal Reference Validation for EB-Cured Polymer Conversions Measured via Raman Spectroscopy. RadTech Rep. 28(4), 46-50.

Schissel, S.M., Lapin, S.C., Jessop, J.L.P., 2017. Characterization and prediction of monomer-based dose rate effects in electron-beam polymerization. Rad. Phys. Chem. Vol 141, 41-49. https://doi.org/10.1016/j.radphyschem.2017.05.028.

Sperling, L.H., 2001. Introduction to Physical Polymer Science, third ed. John Wiley & Sons: New York, pp. 335.

Thiher, N.L.K., Schissel, S.M., Jessop, J.L.P., 2019a. Analysis of methods to determine G-values of monomers polymerized via ionizing radiation. Rad. Phys. Chem. Vol 165, 108394. https://doi.org/10.1016/j.radphyschem.2019.108394.

Thiher, N.L.K., Schissel, S.M., Jessop, J.L.P., 2019b. Counting Radicals: Methods to Measure Radiation Yields of Monomers in EB Polymerization. UV+EB Tech. 5(2), 32-40.

Thiher, N.L.K., Schissel, S.M., Jessop, J.L.P. (2020). The Influence of Monomer Chemistry on Radical Formation and Secondary Reactions During Electron-beam Polymerization. J. Polym. Sci. 58(7), 1011-1021. https://doi.org/10.1002/pol.20190113.

Wilson, J.E., 1974. Radiation chemistry of monomers, polymers, and plastics. Marcel Dekker: New York.

Xianconga, H., Meiwu, S., Guotai, Z., Hong, Z., Xiaopeng, H., Chunlan, Z., 2008. Investigation on the electron-beam curing of vinylester resin. Rad. Phys. Chem. 77(5), 643-655. https://doi.org/10.1016/j.radphyschem.2007.11.006.